

Helioseismology can test the Maxwell-Boltzmann distribution

S. Degl'Innocenti^{1,2,*}, G. Fiorentini^{1,3,†}, M. Lissia^{4,5,‡}, P. Quarati^{6,4,§}, B. Ricci^{1,3,¶}

¹*Istituto Nazionale di Fisica Nucleare, Sezione di Ferrara, via Paradiso 12, I-44100 Ferrara, Italy*

²*Dipartimento di Fisica dell'Università di Pisa, p.zza Torricelli 1, I-56100 Pisa, Italy*

³*Dipartimento di Fisica dell'Università di Ferrara, via Paradiso 12, I-44100 Ferrara, Italy*

⁴*Istituto Nazionale di Fisica Nucleare, Sezione di Cagliari,*

Cittadella Universitaria, I-09042 Monserrato, Italy

⁵*Dipartimento di Fisica dell'Università di Cagliari,*

Cittadella Universitaria, I-09042 Monserrato, Italy

⁶*Dipartimento di Fisica, Politecnico di Torino, I-10129 Torino, Italy*

(8 July 1998)

Abstract

Nuclear reactions in stars occur between nuclei in the high-energy tail of the energy distribution and are sensitive to possible deviations from the standard equilibrium thermal-energy distribution. We are able to derive strong constraints on such deviations by using the detailed helioseismic information of the solar structure. If a small deviation is parameterized with a factor $\exp\{-\delta(E/kT)^2\}$, we find that δ should lie between -0.005 and +0.002. However, even values of δ as small as 0.003 would still give important effects on the neutrino fluxes.

96.06.Jw, 96.60.Ly, 05.20.-y, 26.65.+t

Keywords: Solar interior, helioseismology, statistical mechanics, solar neutrinos

A. Introduction

Thermal averages are fundamental ingredients of the theoretical description of many physical phenomena: solar modeling is a specific example. These thermal averages can and are often described as integrals weighted by the appropriate equilibrium distribution functions; *e.g.*, the mean square averaged velocity $\langle v^2 \rangle$ of a particle in a gas is obtained from the integral of v^2 times the one-body velocity distribution function $f(v)$, the pressure from the integral of pv times $f(v, p)$ (p is the momentum), and so on [1,2].

In the limit of non-interacting states, infinite volume and zero density, a single scale (the temperature or the average one-body energy) characterizes all the equilibrium distributions, which are described by the Maxwell-Boltzmann distribution (MBD). It is well-known that, even for non-interacting states, when the system is finite and/or the density is not zero, the distribution deviates from the MBD, and the resulting distribution (microcanonical, Fermi-Dirac or Bose-Einstein) is characterized by additional scales (total energy, Fermi energy, etc.). Similarly, the interaction could produce additional dynamical scales that modify the free distribution, *e.g.*, ^4He is phenomenologically better described as a weakly-interacting Bose system than in terms of its fermionic constituents. In principle the thermal distribution of the effective weakly interacting degrees of freedom (the bosonic ^4He nuclei, in this example) could be dynamically calculated from the original strong interacting elementary particles (the nucleons). However, theoretical calculations of thermal distribution functions for strongly interacting systems are very difficult, and one often resorts to phenomenologically motivated parameterizations. In specific cases, it has been possible to derive *equilibrium* distributions departing from the MBD [3,4], and, more in general, theoretical frameworks [5–7] have been formulated that naturally produce nonstandard distributions.

In spite of this, one can argue that, even in presence of strong and/or many-body and/or long-range forces, one single scale dominates in many practical case and, therefore, that the MBD is an excellent approximation. This argument is confirmed *a posteriori* by its phenomenological success. However, one should also keep in mind that many applications do not test the details of the distributions, but only one or a few moments. In particular, if a physical quantity is determined by only one moment, one can always summarize the relevant information in the most economical way by using the MBD. In practice, in many cases nothing changes using distributions that differ only in the higher moments. This low sensitivity of many important physical observables to the details of the thermal distribution together with the difficulties of the microscopic calculation leads to the possibility of considering more general distributions that depart from the MBD.

For instance, already two decades ago [8–10] it was proposed that small depletions of the high-energy tail of the relative energy distribution could modify the solar neutrino fluxes. This same idea has been recently reconsidered [11–14] in the light of the new developments that put nonstandard equilibrium distributions on a firmer ground.

Similarly, one could invoke a small enhancement of the high-energy tail of the proton distribution in order to efficiently burn lithium near the bottom of the convective zone. This could be regarded as an attempt to account for the low photospheric lithium abundance (about a factor 100 lower than the meteoric one [15]), essentially unexplained within the Standard Solar Model (SSM) (see, however, Ref. [16]).

In this paper we take the opposite approach and study what kind of constraints our

best knowledge of solar physics, both theoretical and observational, can impose on possible deviations from standard thermal distribution. Our two basic tools will be the sub-barrier fusion reaction rates and helioseismology.

Nuclear reactions in stars occur generally between nuclei with kinetic energy much larger than kT and are thus suitable for probing the high-energy tail of the particle distribution. Even for the pp reaction, which has the lowest barrier, the Gamow peak in the solar core is at energy about five times larger than kT , making the reaction rate very sensitive to changes in number of high-energy particles. Therefore, if we can precisely determine a reaction rate by means of observations, this determination can be used to constrain the particle energy distribution. Stellar interiors are indeed an ideal laboratory for this investigation: they are to a very high degree in thermal equilibrium, and the density is high enough to make deviations from standard statistics conceivable.

Moreover, helioseismology allows us to look deeply in the core of the Sun. The extremely precise measurements of a tremendous number of frequencies enable us to extract values of sound speed with high accuracy even near the solar center [17–22]. In addition several properties of the convective envelope are accurately determined by means of helioseismology.

Recent standard solar models that include the state-of-the-art “standard” solar physics are in good agreement with helioseismic data [17,21,16]. These solar models implicitly assume that the solar core can be described in terms of a gas of particles interacting via two-body forces with no many-body effects apart for mean-field screening. In particular, the ion relative velocity distribution follows the MBD and the diffusion of the average number of particles is Brownian. In some sense, helioseismology tells us that this framework is basically correct. Nevertheless, it is important to quantitatively assess to what extent nonstandard distributions are still compatible with present data. In this respect we remark that *the information on the solar interior provided by helioseismology is so detailed that the pp reaction rate can be reliably constrained* [23].

We shall investigate solar models obtained by modifying a SSM so as to include the effects of a nonstandard distribution. By requiring that the predictions of the resulting solar models agree with the helioseismic determinations of convective envelope properties, we shall constrain the possible nonstandard distributions.

B. Modified statistics and burning rates

In the ordinary treatment, the single particle energy distribution is taken as a MBD for protons and other ions ¹:

$$f_{MBD}(E) = \frac{2}{\sqrt{\pi}} \frac{\sqrt{E}}{(kT)^{3/2}} e^{-E/kT}. \quad (1)$$

The nuclear burning rate between nuclei with mass numbers i and j is given by:

¹In the solar plasma quantum corrections to the statistics are relevant for electrons but not for nuclei.

$$\langle \sigma v \rangle_{ij} = \int d\epsilon \sigma_{ij}(\epsilon) f_{ij}(\epsilon) v(\epsilon), \quad (2)$$

where ϵ is the collision energy, v is the relative velocity, the cross section σ has the usual parameterization

$$\sigma_{ij}(\epsilon) = \frac{S_{ij}}{\epsilon} e^{-bZ_i Z_j \sqrt{\mu/\epsilon}}, \quad (3)$$

and $f_{ij}(\epsilon)$ is the collision-energy distribution of the reacting nuclei. As well known, if the one particle distribution is a MBD, so it is the collision-energy distribution $f_{ij}(\epsilon)$.

Small deviations of $f_{ij}(\epsilon)$ from the MBD can be parameterized to first approximation by introducing a dimensionless parameter δ

$$f_{ij}^{(\delta)}(\epsilon) = f_{MBD}(\epsilon) e^{-\delta(\epsilon/kT)^2}, \quad (4)$$

so that for $\delta=0$ the classical statistics is recovered [9,10,14]; for small δ the distribution is close to the standard one at values of ϵ near the thermal energy kT , whereas significant distortion occurs in the high-energy tail. For $\delta > 0$ this parameterization implies a depletion of the tail. The same parameterization can also be used to mimic an enhanced tail ($\delta < 0$), understanding that a suitable cutoff is introduced [14].

Solar models corresponding to modified statistics have been built by using our stellar evolutionary code FRANEC [24], where all the nuclear-reaction rates have been calculated according to Eqs. (2) and (4). We remark that we are assuming here that δ is the same for every reaction and is constant in the nuclear energy production region ($R/R_\odot \leq 0.2$).

The solar structure is primarily sensitive to the rate of just two reactions:

- i) $p + p \rightarrow d + e^+ + \nu_e$. Since this reaction is at the basis of the nuclear-reaction chain that sustains the Sun against gravitational collapse, it is natural that the internal solar structure is strongly influenced by its rate. As shown in Ref. [23], this rate is strongly constrained by helioseismic determinations of the convective envelope.
- ii) $p + {}^{14}\text{N} \rightarrow {}^{15}\text{O} + \gamma$. The rate of this reaction governs the efficiency of the CNO cycle, which is marginal according to the SSM. An enhancement of the high energy tail ($\delta < 0$) makes the CNO cycle more efficient and even dominant, resulting in solar models drastically different from the SSM (*e.g.*, the energy production is concentrated near the center, a convective core can arise, ...).

C. Modified statistics and the properties of the convective envelope

As shown in Ref. [17], helioseismology determines with high accuracy three independent properties Q of the convective envelope: its depth R_b , the density at its bottom ρ_b and the photospheric helium abundance Y_{ph} .

The helioseismic values of these quantities are shown in Table I together with two estimates of their uncertainties: $(\Delta Q/Q)_{cons}$ corresponds to the (very) conservative definition of Ref. [17], whereas $(\Delta Q/Q)_{1\sigma}$ is the corresponding 1σ “statistical” error estimate.

In the same Table we also show the predictions of the “model with helium and heavy elements diffusion” of Ref. [25] (BP95), which are in excellent agreement with the helioseismic

determinations. For this reason we shall use this model as the reference SSM. As an example of possible “systematic” theoretical uncertainties, we also show results from our solar model including helium and heavy elements diffusion [24] (FR97), which deviates somewhat from the helioseismic determinations.

By numerical experiments with FR97, we have also determined the dependence of these three properties on δ ; results are shown in Fig. 1. The different behavior for negative and positive δ 's becomes more evident as $|\delta|$ increases. This qualitative difference reflects a physical effect: when the tail of the distribution is enhanced ($\delta < 0$) the CNO cycle becomes important (at $\delta = -0.01$ the contributions of the pp-chain and of the CNO cycle are about the same). Since the Gamow energy for the $p + {}^{14}\text{N}$ reaction near the solar center is about 27 keV, a factor five larger than the one for the pp reaction, even a small δ yields drastic effects on the reaction rate and, consequently, on the solar structure.

Nonetheless, for small values of δ , these dependences can be parameterized by power laws:

$$\frac{Q_i}{Q_i^{\text{SSM}}} = \left(e^{-\delta}\right)^{\alpha_{Q_i}}, \quad (5)$$

where the constant exponents α_{Q_i} are shown in the last column of Table I. The solid curves in Fig. 1 demonstrate the goodness of such a parameterization in the range of δ that is relevant to our results ($|\delta| < 0.005$).

Our basic strategy will be the following: *we determine the acceptable range of δ such that R_b , ρ_b and Y_{ph} are predicted within their helioseismic ranges*, by using Eqs. (5) to determine the dependence of these properties on δ .

There are at least four major uncertainties in building standard solar models that also have the potentiality of affecting the three helioseismologic properties under investigation, and, therefore, that could interfere with/hinder the effect of δ : the astrophysical factor S_{pp} , the solar opacity κ , the heavy element abundance $\zeta = Z/X$, and the diffusion coefficients. We shall add all these effects one after the other, and determine a range of δ 's that takes into account these uncertainties.

D. Results

For determining the range of δ allowed by helioseismology, we use several approaches corresponding to increasing conservativeness. We start by defining a χ^2 as:

$$\chi^2(\delta) = \sum_i \left(\frac{Q_i(\delta) - Q_{\odot i}}{\Delta Q_i} \right)^2, \quad (6)$$

where $Q_i(\delta)$ are computed by using Eqs. (5) and the errors are the 1σ estimate of Table I. The value $\chi^2(0)$ indicates how well the SSM reproduces these helioseismic properties. The first row of Table II shows the good agreement between BP95 and helioseismology ($\chi^2/\text{dof} = 8.61/3$).

If we use δ as free parameter (second row of Table II), we find the following best fit value ($\chi^2/\text{dof} = 0.08/2$) and 1σ range:

$$\delta = (-0.77 \pm 0.26) \times 10^{-3}. \quad (7)$$

These strict constraints on the allowed values of δ come mainly from the precise determination of density at the bottom of the convective envelope combined with its strong dependence on δ . In fact, the relative change of Q_i due to $\Delta\delta$ is approximately $\Delta\delta \times \alpha_{Q_i}$; therefore, the allowed variations of δ can be estimated as $\Delta\delta \sim (\Delta Q_i/Q_i)_{1\sigma}/|\alpha_{Q_i}|$ (last column of Table I).

1. Uncertainties on S_{pp}

A conservative estimate of the uncertainty is provided by the range of the published results [26], whereas a 1σ estimate has been provided in [27]; we shall use $\Delta S_{pp}/S_{pp}^{\text{SSM}} = 0.05/3$ at 1σ (5% is the “ 3σ error” estimate). The dependence of Q_i on S_{pp} has been determined numerically in Ref. [23]. By redefining a suitable $\chi^2(\delta, S_{pp})$:

$$\chi^2(\delta, S_{pp}) = \sum_i \left(\frac{Q_i(\delta, S_{pp}) - Q_{\odot i}}{\Delta Q_i} \right)^2 + \left(\frac{S_{pp} - S_{pp, \text{SSM}}}{\Delta S_{pp}} \right)^2, \quad (8)$$

we find that the best fit value of δ does not change and that the 1σ range is double:

$$\delta = (-0.77 \pm 0.50) \times 10^{-3}, \quad (9)$$

and that, consistently, the best fit value for S_{pp} is $S_{pp, \text{SSM}}$. The facts that the SSM is already in very good agreement with helioseismology and that the dependence of the Q_i on S_{pp} is much weaker than that on δ explain these results.

2. Uncertainties on κ and ζ

The heavy element abundance ζ and the solar opacity κ are known with a conservative accuracy of about 10% [28,25,29]. Therefore, our 1σ relative error estimate will be 0.1/3. The dependence² of Q_i on κ and ζ has been determined numerically in Ref. [23]. In this case, the relevant χ^2 is:

$$\chi^2(\delta, S_{pp}, \zeta, \kappa) = \sum_i \left(\frac{Q_i(\delta, S_{pp}, \zeta, \kappa) - Q_{\odot i}}{\Delta Q_i} \right)^2 \quad (10)$$

$$+ \left(\frac{S_{pp} - S_{pp, \text{SSM}}}{\Delta S_{pp}} \right)^2 + \left(\frac{\kappa - \kappa_{\text{SSM}}}{\Delta \kappa} \right)^2 + \left(\frac{\zeta - \zeta_{\text{SSM}}}{\Delta \zeta} \right)^2. \quad (11)$$

We find a small change of the best fit value and, again, an increase of the 1σ range of δ :

$$\delta = (-0.75 \pm 0.67) \times 10^{-3}. \quad (12)$$

Comparing the 3th 4th and 5th row of Table II, one can notice that most of the effect is due to ζ .

²We remark that we are considering a constant rescaling of opacity along the solar profile.

3. Uncertainties on diffusion coefficients

We use a SSM that includes element diffusion, calculated by solving the Burgers equation [30]. Indeed, diffusion has been an essential ingredient of stellar evolutionary codes for achieving agreement between predicted and helioseismic values of properties of the convective envelope [17]. The success of solar models with diffusion, and the corresponding failures of models that neglect diffusion, suggest that the diffusion process has been properly treated. However, in spite of the extensive discussion about the many assumptions underlying the calculation method [31,30,25], no quantitative estimate of the uncertainties of the calculated diffusion coefficients has been presented.

Therefore, we also allow the diffusion efficiency to vary freely by rescaling the diffusion coefficients by an overall constant factor D ($D = 1$ corresponds to the SSM). We have determined the appropriate scaling laws [32] of the properties of the convective zone. For completeness, we report the complete dependence on all the considered quantities (δ , S_{pp} , ζ , κ , and D):

$$\frac{R_b}{R_{b,SSM}} = (e^{-\delta})^{-2.2} \left(\frac{S_{pp}}{S_{pp}^{SSM}} \right)^{-0.058} \left(\frac{\kappa}{\kappa_{SSM}} \right)^{-0.0084} \left(\frac{\zeta}{\zeta_{SSM}} \right)^{-0.046} D^{-0.016} \quad (13a)$$

$$\frac{\rho_b}{\rho_{b,SSM}} = (e^{-\delta})^{33.6} \left(\frac{S_{pp}}{S_{pp}^{SSM}} \right)^{0.86} \left(\frac{\kappa}{\kappa_{SSM}} \right)^{0.095} \left(\frac{\zeta}{\zeta_{SSM}} \right)^{0.47} D^{0.14} \quad (13b)$$

$$\frac{Y_{ph}}{Y_{ph,SSM}} = (e^{-\delta})^{6.2} \left(\frac{S_{pp}}{S_{pp}^{SSM}} \right)^{0.14} \left(\frac{\kappa}{\kappa_{SSM}} \right)^{0.61} \left(\frac{\zeta}{\zeta_{SSM}} \right)^{0.31} D^{-0.091}. \quad (13c)$$

No additional term is added to χ^2 , since we assume that D is completely undetermined (infinite error), and we let it vary freely. The only dependence of χ^2 on D is through $Q_i(\delta, S_{pp}, \zeta, \kappa, D)$. As it is shown in the last row of Table II, the 1σ allowed range becomes:

$$\delta = (-0.91 \pm 1.06) \times 10^{-3}, \quad (14)$$

and we find that the best fit value for D is only 3% smaller than the standard one.

4. Solar model “theoretical uncertainties”

At last we try to estimate how much our results could depend on having used BP95 as reference standard model. To this end, we consider one of the standard solar models (models that include all the state-of-the-art solar physics), whose helioseismic properties differ the most from BP95 and, consequently, fit less well the experimental data. We repeated the above-described analysis by using FR97 as standard solar model. When all parameters are varied, the 1σ range and best fit value, *cf.* Eq. (14), become:

$$\delta = (-1.79 \pm 1.04) \times 10^{-3}. \quad (15)$$

The corresponding fit to the helioseismic properties is acceptable ($\chi^2/\text{dof} = 2.32/1$), the best fit value for D is 9% smaller than the standard one, and the values for ζ and κ are 2% larger.

E. Discussion and conclusions

The constraints we have found on non-Maxwellian statistics look rather strict, as the dimensionless parameter cannot exceed a few per thousand. In fact, if we define a conservative interval as the union of the 3σ ranges found by using BP95 and FR97 SSMs, we find

$$-4.9 \times 10^{-3} < \delta < 2.3 \times 10^{-3}. \quad (16)$$

However, even these small values of δ could have non-negligible implications for those observables that are sensible to the high-energy tail of the distribution. As an example, we have estimated the possible effects of $\delta = \pm 3 \times 10^{-3}$ in the two cases mentioned in the introduction.

1. Neutrino fluxes

In Table III, we report the effect of nonstandard statistics on the main fluxes and on the signals of the chlorine and gallium radiochemical experiments. Even for such small values of δ the *boron and beryllium fluxes change substantially*.

2. Lithium abundance

As well known, the photospheric abundance of lithium is a factor about 100 lower compared to the meteoric one [15]. Different mechanisms have been proposed to explain this depletion [16,33,34]. Let us discuss the possibility that nonstandard velocity distribution could contribute to this depletion. First of all we note that, since the lithium abundance should be reduced in order to solve/alleviate the problem, the lithium burning rate should be enhanced relative to the standard case. This is achieved by a longer high-energy tail, *i.e.*, $\delta < 0$.

We assume that the limits on δ derived in the production region apply also up to the bottom of the convective zone, and consider $\delta = -3 \times 10^{-3}$. This value of δ yields a reduction of the ${}^7\text{Li}$ abundance by only 7%, where the characteristics of the bottom of the convective zone has been taken from FR97 ($T_b = 2.1 \times 10^6$ K, $\rho_b = 0.18$ g/cm 3 and $X = 0.744$). Depletions comparable with the observed ones could be obtained with $\delta \sim -0.15$, a value well outside the range reported in Eq. (16).

REFERENCES

- * Electronic address: scilla@astr18pi.difi.unipi.it
 - † Electronic address: fiorentini@fe.infn.it
 - ‡ Electronic address: marcello.lissia@ca.infn.it
 - § Electronic address: quarati@polito.it
 - ¶ Electronic address: ricci@fe.infn.it
- [1] L. D. Landau and E. M. Lifshitz, *Statistical Physics, Part 1* (Pergamon Press, Oxford, 1980)
 - [2] K. Huang, *Statistical Mechanics* (John Wiley & Sons, Inc., New York, 1963); 2nd Edition (1987).
 - [3] G. Kaniadakis and P. Quarati, *Physica A* 192 (1993) 677.
 - [4] G. Kaniadakis and P. Quarati, *Physica A* 237 (1997) 299.
 - [5] C. Tsallis, *J. Stat. Phys.* 52 (1998) 479.
 - [6] E. M. F. Curado and C. Tsallis, *J. Phys. A* 24 (1991) L69; *ibid.* 24 (1991) 3187(E); *ibid.* 25 (1992) 1019(E).
 - [7] C. Tsallis, *et al.*, *Phys. Rev. Lett.* 75 (1995) 3589; *ibid.* 77 (1996) 5442(E).
 - [8] S. Vasil'ev, G. Kocharov, and A. Levkovskii, *Izv. AN SSSR, Ser. Fiz.* 38 (1974) 1827; *ibid.*, 39 (1975) 310.
 - [9] D. D. Clayton, *Nature* 249 (1974) 131.
 - [10] D. D. Clayton, E. Eliahu, M. J. Newman, and R. J. Talbot, Jr., *Astrophys. J.* 199 (1975) 494.
 - [11] H. Haubold and A. M. Mathai, *Astrophys. Space Sci.* 228 (1995) 77; *ibid.*, 228 (1995) 113.
 - [12] G. Kaniadakis, A. Lavagno, and P. Quarati, *Phys. Lett. B* 369 (1996) 308.
 - [13] P. Quarati, A. Carbone, G. Gervino, G. Kaniadakis, A. Lavagno, and E. Miraldi, *Nucl. Phys. A* 621 (1997) 345c.
 - [14] G. Kaniadakis, A. Lavagno, M. Lissia, and P. Quarati, astro-ph/9710173 (1997).
 - [15] E. Anders and N. Grevesse, *Geochimica and Cosmochimica Acta* 53 (1989) 197.
 - [16] O. Richard, S. Vauclair, C. Charbonnel, and W. A. Dziembowski, *Astron. Astrophys.* 312 (1996) 1000.
 - [17] S. Degl'Innocenti, W. A. Dziembowski, G. Fiorentini, and B. Ricci, *Astr. Phys.* 7 (1997) 77.
 - [18] S. Basu and M. J. Thompson, *Astr. Astroph.* 305 (1996) 631.
 - [19] S. Basu, J. Christensen-Dalsgaard, *Astr. Astroph.* 322 (1997) L5.
 - [20] D. O. Gough, *et. al.*, *Science* 272 (1996) 1296.
 - [21] J. N. Bahcall, M. H. Pinsonneault, S. Basu, and J. Christensen-Dalsgaard, *Phys. Rev. Lett.* 78 (1997) 171.
 - [22] W. A. Dziembowski, P. R. Goode, A. A. Pamyatnykh and R. Sienkiewicz, *Ap. J.* 432 (1994) 417.
 - [23] S. Degl'Innocenti, G. Fiorentini, and B. Ricci, *Phys. Lett. B* 416 (1998) 365.
 - [24] S. Degl'Innocenti, F. Ciacio, and B. Ricci, *Astr. Astroph. Suppl. Ser.* 123 (1997) 1.
 - [25] J. N. Bahcall and M. H. Pinsonneault, *Rev. Mod. Phys.* 67 (1995) 781.
 - [26] Private communication by NACRE collaboration (1998), to appear within the publication plane of the collaboration.

- [27] M. Kamionkowski and J. N. Bahcall, Ap. J. 420 (1994) 884.
- [28] J. N. Bahcall and M. H. Pinsonneault, Rev. Mod. Phys. 64 (1992) 885.
- [29] V. Castellani, S. Degl'Innocenti, G. Fiorentini, M. Lissia and B. Ricci, Phys. Rep. 281 (1997) 309.
- [30] A. A. Thoul, J. N. Bahcall, and A. Loeb, Ap. J. 421 (1994) 828.
- [31] A. N. Cox, J. A. Guzik, and R. B. Kidman, Astrophys. J. 342 (1989) 1187, and Refs. therein.
- [32] B. Ricci, *et al.*, in preparation.
- [33] V. Castellani, G. Fiorentini, O. Straniero, and B. Ricci, Z. Phys. A 354 (1996) 237.
- [34] B. Chaboyer, P. Demarque, and M. H. Pinsonneault, Ap. J. 441 (1995) 865.

TABLES

TABLE I. The three independent properties of the convective envelope used in our analysis. The first column (Q_i) labels the property, the second (BP95) and third (FR97) columns show the values predicted by the reference solar model BP95 [25] and by FR97 [24] standard model, the fourth column ($Q_{i\odot}$) shows the value derived by helioseismic measurements, and the next two columns the corresponding conservative and 1σ errors. The last two columns show the exponents that determine the dependence from δ , $\alpha_{Q_i} \equiv -d \log Q_i / d\delta$, and the ratios between the 1σ error and $|\alpha_{Q_i}|$ (see text).

Q_i	BP95	FR97	$Q_{i\odot}$	$(\Delta Q_i / Q_i)_{\text{cons}}$	$(\Delta Q_i / Q_i)_{1\sigma}$	α_{Q_i}	$(\Delta Q_i / Q_i)_{1\sigma} / \alpha_{Q_i} \times 10^3$
Y_{ph}	0.24695	0.2321	0.249	0.042	0.014	6.2	2.2
R_b / R_\odot	0.712	0.715	0.711	0.004	0.002	-2.2	0.9
ρ_b [g/cm ³]	0.187	0.182	0.192	0.037	0.0094	33.6	0.3

TABLE II. Deviations from standard statistics allowed by helioseismic measurements. The first five columns show whether the parameter is kept fixed (F) at its SSM value or it is allowed to vary (V) as a free parameter within the range discussed in the text. The sixth column shows the resulting χ^2 per degree of freedom. The last two columns show the best fit value for δ and its 1σ error.

D	κ	ζ	S_{pp}	δ	χ^2/dof	$\delta_{\text{Best}} \times 10^3$	$\Delta\delta$
F	F	F	F	F	8.61 /3		
F	F	F	F	V	0.08 /2	-0.77	0.26
F	F	F	V	V	0.08 /2	-0.77	0.50
F	F	V	V	V	0.08 /2	-0.73	0.67
F	V	V	V	V	0.04 /2	-0.75	0.67
V	V	V	V	V	0.001/1	-0.91	1.06

TABLE III. Effects of nonstandard statistics on neutrino fluxes. Relative deviations from SSMs of the ⁷Be and ⁸B neutrino fluxes and of the expected signals for gallium and chlorine detectors in two nonstandard solar models with deformed velocity distribution ($\delta \neq 0$).

	$\delta = +3 \times 10^{-3}$	$\delta = -3 \times 10^{-3}$
$\Delta\Phi_{\text{Be}}/\Phi_{\text{Be}}$	-0.30	+0.38
$\Delta\Phi_{\text{B}}/\Phi_{\text{B}}$	-0.55	+1.15
$\Delta S_{\text{Cl}}/S_{\text{Cl}}$	-0.16	+0.31
$\Delta S_{\text{Ga}}/S_{\text{Ga}}$	-0.50	+1.03

FIGURES

FIG. 1. Dependence on δ of the three independent properties of the convective envelope used in our analysis. Crosses show the values of the photospheric helium abundance Y_{ph} (a), the density at the bottom of the convective envelope ρ_b (b), and the depth of this envelope R_b (c), relative to their standard values, as functions of δ . The solid curves are the fits in Eq. (5) with the exponents α_{Q_i} from the second last column of Table I.

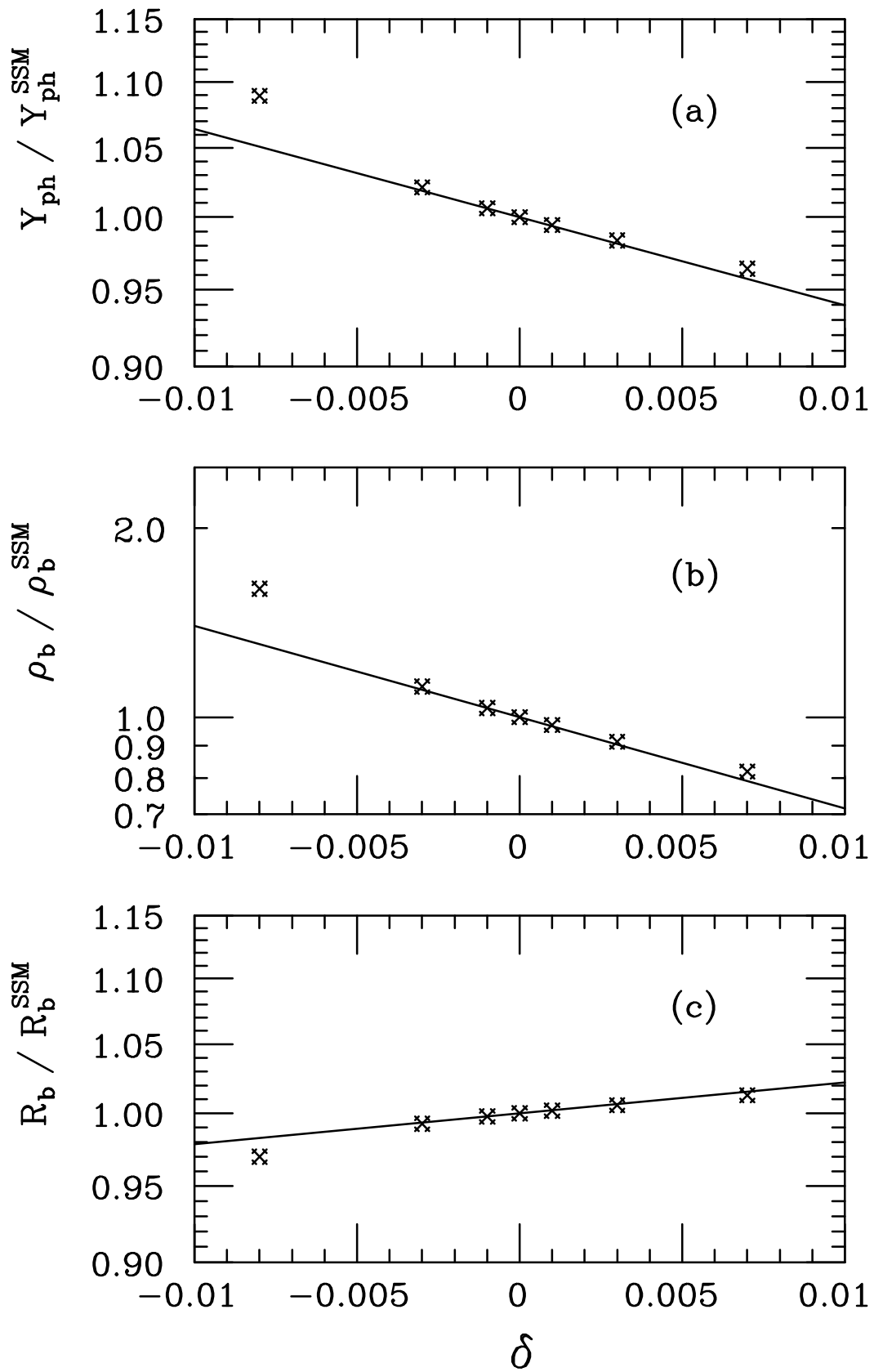


Fig. 1 From: Degl'Innocenti et al.
 Helioseismology can test the ...